

# The functionalization of magnetite nanoparticles by hydroxyl substituted diazacrown ether, able to mimic natural siderophores, and investigation of their antimicrobial activity

Ulviyya Alimammad Hasanova<sup>1</sup> · Mahammadali Ahmad Ramazanov<sup>1</sup> ·  
Abel Mammadali Maharramov<sup>1</sup> · Zarema Gakhramanova<sup>2</sup> · Sarvinaz Faiq Hajiyeve<sup>1</sup> ·  
Leyla Vezirova<sup>2</sup> · Goncha Malik Eyvazova<sup>1</sup> · Flora Vidadi Hajiyeve<sup>1</sup> ·  
Parvana Huseynova<sup>2</sup> · Zohrab Agamaliyev<sup>1</sup>

Received: 30 November 2015 / Accepted: 1 July 2016 / Published online: 9 July 2016  
© Springer Science+Business Media Dordrecht 2016

**Abstract** In this work we report of functionalization of magnetite nanoparticles by hydroxyl containing diaza-crown ether—macroheterocycle (MC) that is able to mimic the properties of natural siderophores. The structure of synthesized crown ether was investigated by NMR, mass-, FTIR spectroscopy methods. The morphology of prepared MC@Fe<sub>3</sub>O<sub>4</sub> nano-ensembles was analysed by scanning electron microscopy SEM, X-ray diffraction XRD analysis methods. The quantitative analysis of nanostructures was determined by atom absorbance spectroscopy as well as on the basis of Lambert–Beer law by UV spectroscopy method. It was found that the synthesized compounds were effective against gram-negative microorganisms *Escherichia coli*, *Klebsiella spp.* and gram-positive *Staphylococcus aureus*, having multi drug resistance properties.

**Keywords** Macrocycles · Crown ether · Supramolecular chemistry · Siderophores · Magnetite nanoparticles

## Introduction

In the last decades supramolecular chemistry and nanotechnology become to develop quickly and spread into different areas of science. Conceptually supramolecular chemistry and nanotechnology have much in common, as the formation of nanostructures is based on the principle of self-assembly and self-organization and that is the essence of supramolecular ensembles. Supramolecular structures play a vital role in functioning of living organism. Their unique feature is that they arise spontaneously, via hydrophobic interactions, electrostatic effects that in turn arise from the interaction of functional groups of biomolecules with an aqueous environment and through non-covalent bonds that play important role in the formation of these structures [1]. All these naturally occurring supramolecular compounds, forming via self-assembling, are designed for realization of vital biological functions of living organisms [2].

✉ Mahammadali Ahmad Ramazanov  
mamed\_r50@mail.ru

Ulviyya Alimammad Hasanova  
ulviyya3@rambler.ru

Abel Mammadali Maharramov  
rector@bsu.az

Zarema Gakhramanova  
u.alimammad@gmail.com

Sarvinaz Faiq Hajiyeve  
sarvinazhajiyeve@gmail.com

Leyla Vezirova  
mamed\_r44@rambler.ru

Goncha Malik Eyvazova  
eygoncha@gmail.com

Flora Vidadi Hajiyeve  
flora\_1985@mail.ru

Parvana Huseynova  
nanomaterials@bsu.edu.az

Zohrab Agamaliyev  
a-zohrab@hotmail.com

<sup>1</sup> Nano Research Laboratory, Baku State University,  
Z. Khalilov 23, AZ1148 Baku, Azerbaijan

<sup>2</sup> RI Geotechnological problems of gas oil and chemistry,  
Azerbaijan State University of Oil and Industry, Baku,  
Azerbaijan

So, synthetic analogues of such systems are very interesting, in term of its supramolecular properties, imitating the properties of naturally occurring systems. The crown ethers can demonstrate the properties of naturally occurring membrane active antibiotics, thanks to ionophore feature of macrocycle cavity to bind the cations through ion-dipole, dipole–dipole non-covalent bonds. [3] After the binding, the ionophore antibiotics, such as valinomycin and nonactin, drag ions into the bacterial cell, change the permeability of the membrane and disrupt the oxidative phosphorylation. [4] Azacrown ethers, cryptands, thiacycrown ethers and their derivatives, having nitrogen, sulphur atoms in macrocyclic ring, are able to selectively bind to metal ions. The substitution of macrocycle's oxygen atoms by nitrogen atoms increases the complex formation ability, as the nitrogen atoms are softer bases. Azacrown ethers are able to bind the ions of transfer and rare earth metals. [5] Beside this, the synthesis of macroheterocycles, having various functional groups in their molecule, notably influences on the ability of these compounds to form supramolecular ensembles by means of non-covalent interactions [6].

At the same time the potential applications of nanomaterial in biomedicine field attract more attention in modern science. The magnetite nanoparticles have already shown promising results in preclinical experiments for imaging contrast enhancement, tissue repair, magnetic hyperthermia and drug delivery [7–10]. In this regard, the combination of two perspective approaches in designing new drugs can be very useful, due to the new advantages, created by unique features of both nanoparticles and supramolecular compounds. So, the functionalization of magnetite nanoparticle with hydroxyl substituted diazacrown ether, able to mimic natural siderophores, is a matter of great scientific and practical interest.

## Materials and methods

All chemicals, used in the synthesis, were of analytical grade and used as received. Ethylenediamine, 1,3-dichloro-2-propanol, salysilaldehyde were purified by distillation under reduced pressure, created by water pump.  $\text{FeCl}_3 \cdot 6\text{H}_2\text{O}$ ,  $\text{FeSO}_4 \cdot 7\text{H}_2\text{O}$ ,  $\text{NH}_4\text{OH}$  (25 %), were purchased from Sigma-Aldrich (Taufkirchen, Germany); Nutrient Broth was purchased from Biolife (Milano, Italia).

### Synthesis of (4) MC 1,13-Diaza-5,9-dioxa-7-hydroxy-3,4:10,1-dibenzocyclopentadecan

#### Preparation of MC-general procedure

The ethylenediamine (0.003 mol), dissolved in 20 cm<sup>3</sup> of methanol, was added dropwise to salysilaldehyde (1)

(0.003 mol) in 150 cm<sup>3</sup> of methanol. After the addition, the reaction mixture was stirred to room temperature, and 0.006 mol of sodium borohydride in 15 mL of dimethyl formamide was added in portions with stirring. The yellow colour of the reaction mixture disappears with addition of all portion of sodium borohydride, indicated to completion of hydrogenation. When the reduction was completed, mixture was poured in cold distilled water. Formed white precipitate was washed with water and diethyl ether, and then dried over anhydrous sodium sulphate.

Yield of (3) 0.57 g (70 %), m.p. 122–124 °C. Found: C 70.62, H 7.39, N 10.26. Calc. For  $\text{C}_{16}\text{H}_{20}\text{O}_2\text{N}_2$ : C 70.59, H 7.35, N 10.29 %. NaOH, dissolved in 0.1 cm<sup>3</sup> of water was added to (3) (0.003 mol) in 150 cm<sup>3</sup> of n-butanol (0.006 mol). The reaction mixture was heated and then (0.003 mol) of 1,3-dichloro-2-propanol, dissolved in 15 cm<sup>3</sup> of n-butanol, was added dropwise during 30 min. Reaction mixture was stirred and refluxed 30 h. When the reaction was completed, the mixture was filtered, and then the filtrate was evaporated to minimum volume. The residue was dissolved in 50 cm<sup>3</sup> of water and extracted with chloroform (3 × 50 cm<sup>3</sup>). Removal of the solvent gave the product (4). The further purification was carried by recrystallization from mixture butanol-1:toluene, yield 0.70 g (65 %), m.p. 148–149 °C. Found: C 69.5, H 7.4, N 8.7. Calc. for  $\text{C}_{19}\text{H}_{24}\text{N}_2\text{O}_3$ : C 69.5, H 7.4, N. 8.5 %. IR (KBr): 3350 (OH); 3330, 1455 (NH); 1604, 1590, 1492 (Ar); 1255, 1035 (Ar–O–CH<sub>2</sub>); 754 (1,2-Ar) cm<sup>-1</sup>. <sup>1</sup>H NMR ( $\delta$ ): 2.64 (s, 4H, NCH<sub>2</sub>CH<sub>2</sub>N), 3.24 (br, 3H, NH and OH), 3.65 (s, 4H, ArCH<sub>2</sub>), 4.14 (m, 5H, CH<sub>2</sub>CHCH<sub>2</sub>), 6.74–7.25 (m, 8H, ArH) ppm.

### Synthesis of nanostructures by functionalization of Fe<sub>3</sub>O<sub>4</sub> with MC (MC@Fe<sub>3</sub>O<sub>4</sub> NPs)

Magnetic iron oxide nanoparticles are usually prepared by wet chemical precipitation from aqueous iron salt solutions in alkaline milieu, created by using  $\text{NH}_4\text{OH}$ , in the atmosphere of gaseous nitrogen. [11] The formed  $\text{Fe}_3\text{O}_4$  nanoparticles (NPs) were separated by strong NdFeB permanent magnet, repeatedly washed with distilled water and dispersed in ethanol. The ethanol solution of MC, taken in excess, was added to ethanol solution of  $\text{Fe}_3\text{O}_4$  nanoparticles and vigorously stirred. After stirring during 8 h at ambient, the prepared nanostructures were separated by strong NdFeB permanent magnet and repeatedly were washed with distilled water. The obtained NPs were dried at ambient conditions and the iron content in the samples was analyzed by atom absorption spectroscopy and performed on Varian SpectraAA 220FS Atomic absorption spectrometer. Samples were prepared by Milestone ETHOS 1 Microwave extraction unit. The UV spectra have been recorded on Spectrophotometer specord 250 Plus. UV

spectra were recorded at the range 275 nm for standard solutions of MC.

## Characterization of structure

### XRD

X-ray diffraction analysis was performed on Rigaku Mini Flex 600 XRD diffractometer at ambient. In all the cases, Cu K  $\alpha$  radiation from a Cu X-ray tube (run at 15 mA and 30 kV) was used. The samples were scanned in the Bragg angle  $2\theta$  range of 20–70°.

### FT-IR

The functional groups, present in the powder samples of MC@Fe<sub>3</sub>O<sub>4</sub> NPs, were identified by Fourier Transform Infrared (FTIR) spectroscopy. FTIR spectra were recorded on a Varian 3600 FTIR spectrophotometer in KBr tablets. The spectrum was taken in the range of 4000–400 cm<sup>−1</sup> at room temperature, with resolution 4 cm<sup>−1</sup> and scan number 32.

### Scanning electron microscope (SEM) and energy-dispersive spectrum (EDS) analysis

SEM and EDS analysis of prepared samples of MC@Fe<sub>3</sub>O<sub>4</sub> nanoparticles were taken on Field Emission Scanning Electron Microscope JEOL JSM-7600F at an accelerating voltage of 15.0 kV, SEI regime.

### Determination of antibacterial activity

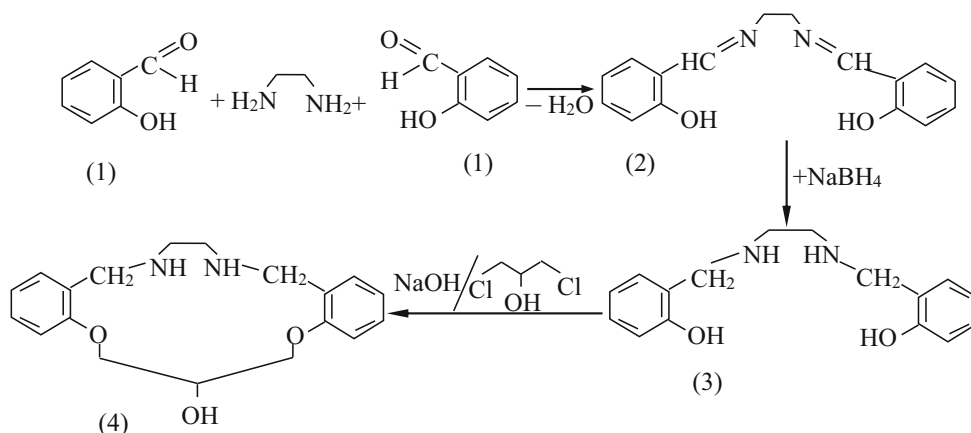
Antibacterial activity of MC and MC@Fe<sub>3</sub>O<sub>4</sub> was tested by diffusion method, performed on Petri dishes, on *Staphylococcus aureus*, *Klebsiella spp.* and *Escherichia coli*. [12] The synthesized substances were taken in amount equal to 30  $\mu$ g. *Escherichia coli* were cultivated on Endo's

medium, *K. spp.* on Sabouraud medium and *S. aureus* on Baird–Parker agar (cultures were kindly provided by one of the clinical laboratories of Baku). Due to the fact that this method provides only quality data, microdilution method was also performed. By this method the minimal inhibitory concentration (MIC) of prepared substances on *S. aureus*, *K. spp.* and *E. coli* was identified. To perform microdilution method the stock solutions of different concentrations of the substances were prepared in distilled sterile water and distributed in 96 multi-well plates. Each well was inoculated with 0.1 mL of microbial suspensions of 0.5 McFarland turbidity, prepared from 24 h fresh culture. Sterility control wells (nutrient broth) and microbial growth controls (inoculated nutrient broth) were used. The plates were incubated for 24 h at 37 °C [12] [13]. In order to measure antibacterial effect on biofilm development, the nutrient broth was deleted; wells were washed with PBS three times, dried 15 min in room temperature and stained by crystal violet 1 % for 15 min. After the deletion of crystal violet 1 %, wells again were washed 3 times with PBS 3 times and dried at room temperature for 15 min. Further, the biofilm, formed onto the plastic wells, was re-suspended in 30 % acetic acid and the intensity of the coloured suspension was assayed by measuring the absorbance at 590 nm [9, 14, 15].

## Results and discussions

Synthesis of MC 1,13-Diaza-5,9-dioxa-7-hydroxy-3,4:10,11-dibenzocyclopentadecane(4) is shown on the Scheme 1. N,N' ethylene bis (salysilimine) (2) was prepared by condensation of salicylaldehyde (1) with ethylenediamine. The reduction of (2) was carried out by sodium borohydride. The ring closure step was carried out by reaction of corresponding saturated derivative (3) with 1,3-dichloro-2-propanol. Then magnetite nanoparticles were functionalized by synthesized MC via non-covalent

**Scheme 1** The synthesis of MC 1,13-Diaza-5,9-dioxa-7-hydroxy-3,4:10,11-dibenzocyclopentadecane



interactions occurring between the surface of nanoparticles and functional groups of MC.

The purity and crystalline properties of the MC@Fe<sub>3</sub>O<sub>4</sub> were investigated by powder X-ray diffraction (XRD). The XRD patterns are shown in Fig. 1. All the XRD peaks were well defined and corresponded to Fe<sub>3</sub>O<sub>4</sub> nanoparticles with cubic structure. In XRD peak broadening testifies for the formation of nanocrystals. In the pattern all lines relate to magnetite and can be indexed, using the ICDD (PDF-2/Release 2011 RDB) DB card number 00-001-1111, for prepared nanostructure. The pattern of MC@Fe<sub>3</sub>O<sub>4</sub> NPs has characteristic peaks at 30.25° (220), 35.75° (311), 43.52° (400), 57.44° (511), 62.93° (440) Table 1 and that correlates with the standard pattern of Fe<sub>3</sub>O<sub>4</sub> well. The intensity of the diffraction peak of (311) plane is stronger than the other peaks. The average crystal size, estimated from (311) peak, using the Scherrer formula, is 14.8 nm for MC@Fe<sub>3</sub>O<sub>4</sub> pattern nanoparticles.

Figure 2 presents the FTIR spectra of pristine MC (1), MC@Fe<sub>3</sub>O<sub>4</sub> (2) and pristine magnetite (3). The spectra of prepared nanostructures were compared with spectra of pristine MC and spectra of pristine Fe<sub>3</sub>O<sub>4</sub>, in order to determine the coordination sites of MC that may be involved in chelation with surface of magnetite nanoparticles. The spectrum of nanostructures' samples (2) reveals the characteristic peak of Fe<sub>3</sub>O<sub>4</sub> at about 575 cm<sup>-1</sup> corresponding to (Fe–O stretching). The comparison of spectrum of pure MC with spectrum of prepared nanostructures shows the weakening of intensity of strong band at 1455 cm<sup>-1</sup>, corresponding to the NH groups in the nanostructures. At the same time the wide band at 3330–3350 cm<sup>-1</sup>, corresponding to ν(OH) and ν(NH) in pristine MC, disappears in the spectrum, corresponded to nanostructures Fig. 2 (2), and that is strong evidence of

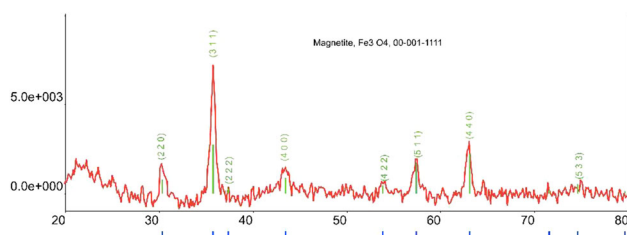


**Fig. 1** XRD pattern for the nanostructured MC@Fe<sub>3</sub>O<sub>4</sub> NPs

**Table 1** XRD Peak list for MC@Fe<sub>3</sub>O<sub>4</sub> NPs

No.	2-theta(deg)	d(ang.)	Height(cps)	Int. I(cps deg)	Int. W(deg)	Asym. factor	Size(ang.)
1	30.2518	2.952	1517.04	721.513	0.475607	1.96336	145.542
2	35.75 (5)	2.509 (3)	4327 (85)	3054 (225)	0.71 (7)	2.0 (8)	148 (11)
3	43.5252	2.07761	1286.25	618.019	0.480480	1.96336	151.282
4	57.446	1.60286	1744.65	851.951	0.488323	1.96336	160.214
5	62.93 (7)	1.4756 (15)	1953 (57)	1286 (138)	0.66 (9)	1.5 (8)	166 (16)

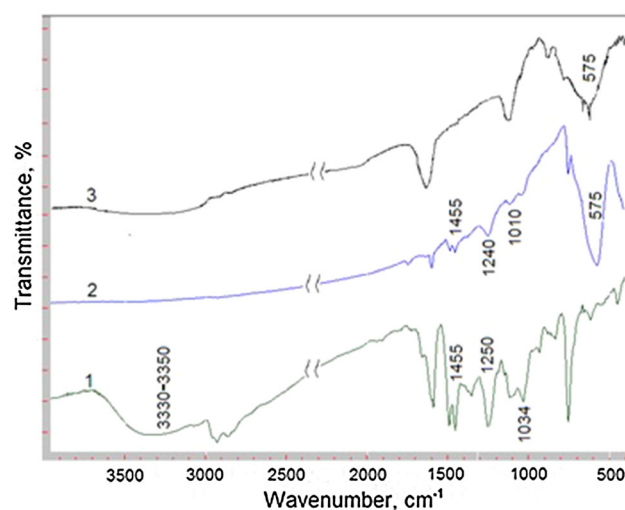


**Fig. 2** FTIR spectra (1) pristine MC, (2) MC@Fe<sub>3</sub>O<sub>4</sub>, (3) pristine Fe<sub>3</sub>O<sub>4</sub>

coordination of MC molecules with magnetite surface via OH and NH groups of MC. The intense band at 1250 and 1034 cm<sup>-1</sup> (Ar–O–CH<sub>2</sub>) of MC Fig. 2 (1) is shifted to 1240 and 1010 cm<sup>-1</sup> region in the spectra of MC@Fe<sub>3</sub>O<sub>4</sub>. These indicate the involving of macrocycle's oxygen atoms in coordination process.

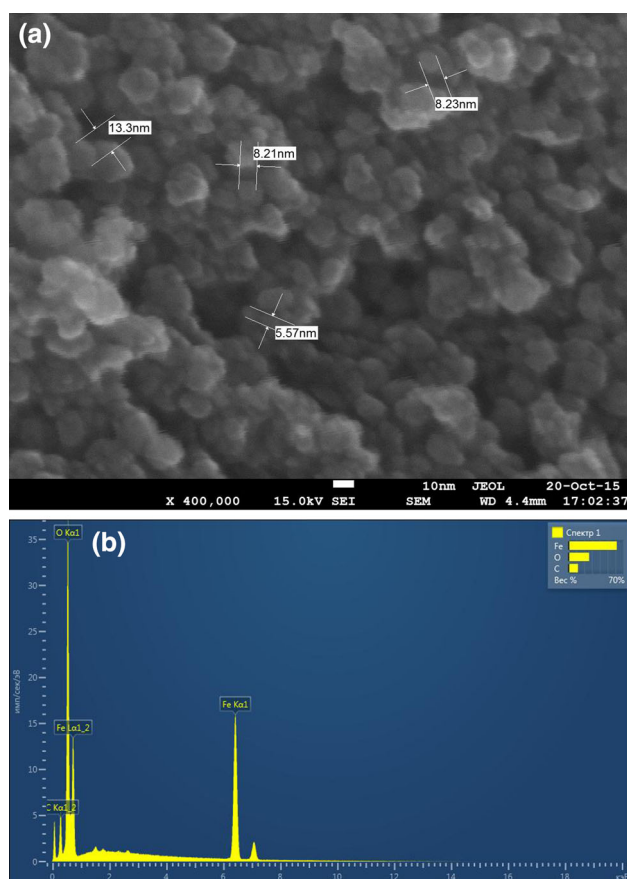
As it seen from FTIR spectra, the absorption occurs through NH, OH and macrocycle's oxygen atoms by self-assembling via non-covalent interaction with surface of magnetic NPs. Thus, the IR spectral results provide strong evidences for the multiple chelation sites of MC and drugs molecules with surface of magnetite NPs.

The prepared nanostructures were analysed by SEM and EDS, and the results are presented on Fig. 3. As it seen from Fig. 3(a), the obtained nanoparticles are homogenous and the size of nanostructures varies in the range from 8 to 15 nm and this very well correlates with the results, obtained from XRD analysis.

The points, identified in the EDS spectra Fig. 3(b), demonstrate the presence of Fe and O as the main elements of the sample and support the data of magnetite nanoparticles formation (the other peaks are corresponding to Cu and C, being characteristic of the carbon-coated grid).

The synthesized MC has high absorption peak in the UV spectrum, observed at the 275 nm. This fact allows quantitatively determining the amount of absorbed MC on

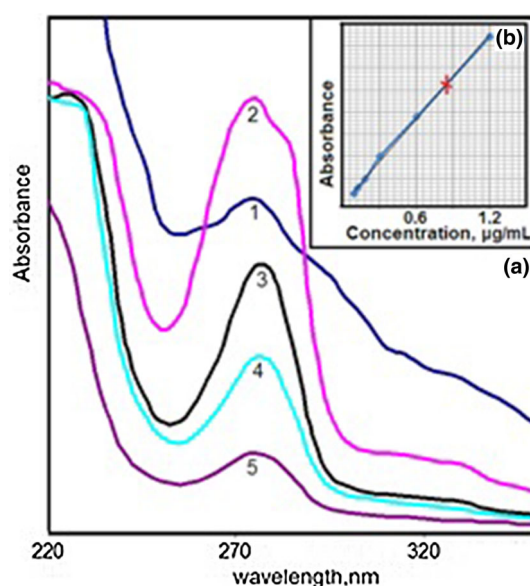




**Fig. 3** **a** SEM image of MC@Fe<sub>3</sub>O<sub>4</sub> NPs; **b** ED pattern of MC@Fe<sub>3</sub>O<sub>4</sub> NPs

Fe<sub>3</sub>O<sub>4</sub> NPs. Figure 4 shows the UV spectrum of a standard ethanol solution of pure MC (Fig. 4 (2–5)) and preliminarily sonicated ethanol solution of precise weighted amount of MC@Fe<sub>3</sub>O<sub>4</sub> NPs (Fig. 4 (1)). UV spectra were recorded at 275 nm for standard solutions of MC with different concentrations in the range of 0.15–1.2 µg/mL (Fig. 4). Quantitative analysis of absorbed MC onto surface of magnetite nanoparticles was determined by spectroscopic method on the basis of Lambert–Beer law. Atom absorption spectroscopy method also was applied for determination of quantity of absorbed MC molecules. At the same time, by AAS method was determined the iron content in the sample of prepared nanostructures. The further calculations allow defining the amount of the actual MC in the samples. It was found that 1 g of MC@Fe<sub>3</sub>O<sub>4</sub> NPs contains 0.21 g of MC. The obtained data from two methods of quantitative analysis correlate to each other very well.

The obtained nanostructures were expected to reveal the biological activity against microorganisms, so they were tested toward gram-positive bacteria *S. aureus* and gram-negative bacteria *E. coli* and *K. spp.* We assumed that the

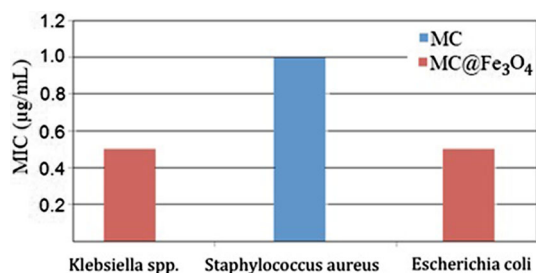


**Fig. 4** UV spectra of MC@Fe<sub>3</sub>O<sub>4</sub> (1) found 0.087 µg/mL; pure MC; (2) 1.2 µg/mL; (3) 0.6 µg/mL; (4) 0.3 µg/mL; (5) 0.15 µg/mL

synthesized MC would be able to reveal antimicrobial activity due to ionophoric properties as well as MC@Fe<sub>3</sub>O<sub>4</sub> nanostructures can mimic the properties of natural siderophores, especially in case of gram-negative microorganisms. The results of the microdiffusion method show that the inhibition zone, produced by MC on *S. aureus*, was 14 mm in diameter, but there was no effect on *E. coli* and *K. spp.* However, when it comes to MC@Fe<sub>3</sub>O<sub>4</sub>, the contrary results were observed. It has no effect on *S. aureus*, but has produced an inhibition zone with the diameter 28 mm on *E. coli* and 22 mm on *K. spp.* (Table 2). The antibacterial effect of MC on *S. aureus* can be explained by the fact that it acts like ionophore, disrupting the membrane's potential of bacteria. [16] At the same time, in case of MC@Fe<sub>3</sub>O<sub>4</sub>, antibacterial effect is absent, probably, because Fe<sub>3</sub>O<sub>4</sub> NPs blocked action sites of crown ethers, responsible for ionophore binding with membrane via OH, NH and MC' oxygen atoms by means of ion-dipole, dipole-dipole and etc. interactions. When it comes to *E. coli* and *K. spp.*, we can suppose that the mechanism is quite different. As it is known, gram-negative bacteria form so called siderophoric system that can acquire iron from the environment by secreting special iron-chelating agents—siderophores. These siderophores penetrate to periplasmic space through responsible for iron uptake porin channels. [17] We can assume that hydroxyl substituted diazacrown ether is similar to siderophores in their ability to chelate iron. MC alone cannot penetrate through the thick membrane of gram-negative bacteria and exhibit antibacterial effect; however, laden with iron, it plays a role as a siderophore and more likely is more advantageous for bacterial cells

**Table 2** The diameter of inhibition zones, produced by MC and MC@Fe<sub>3</sub>O<sub>4</sub>, on *Escherichia coli*, *Staphylococcus aureus* and *Klebsiella spp.*

	<i>Escherichia coli</i>	<i>Staphylococcus aureus</i>	<i>Klebsiella spp.</i>
MC	–	14 mm	–
MC@Fe <sub>3</sub> O <sub>4</sub>	28 mm	–	22 mm

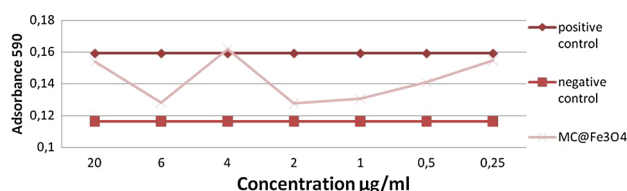
**Fig. 5** The graphic representation of the MIC (µg/mL) of MC@Fe<sub>3</sub>O<sub>4</sub> and MC against *Klebsiella spp.*, *Staphylococcus aureus* and *Escherichia coli*

than natural free-from-iron siderophore. In our opinion, the sum of all above-mentioned factors contributes to high antimicrobial effect of MC@Fe<sub>3</sub>O<sub>4</sub> on gram-negative bacteria.

Further the broth microdilution method was assayed, and from its results was observed that the minimal inhibition concentration MIC of MC@Fe<sub>3</sub>O<sub>4</sub> NPs on *K. spp.* was equal to 0.5 µg/mL. On *S. aureus* the MIC of MC was equal to 1 µg/mL. In case of *E. coli*, the MC@Fe<sub>3</sub>O<sub>4</sub> NPs' MIC is 0.5 µg/mL (Fig. 5).

Moreover, MC@Fe<sub>3</sub>O<sub>4</sub> exhibited inhibitory effect on biofilm development of *K. spp.* almost in all concentrations from 20 to 0.5, demonstrating that the loading of crown ether into magnetic nanoparticles provides an improved delivery of the active compound to the bacterial target, even when it grows in biofilm (Fig. 6).

According to the spectra, in case of *S. aureus*, MC does not exhibit an inhibitory effect on biofilm development. We can suppose that it is connected with the possible non-covalent interactions of MC with main constituents of biofilm such as DNA fragments, polysaccharides' matrix and specific proteins. [18] So, it does not even reach to the bacterial cells, situated in biofilm.

**Fig. 6** The graphic representation of *Klebsiella spp.*'s biofilm development in the presence of nano crown ether

We suppose that when azacrown ether bind to the Fe<sub>3</sub>O<sub>4</sub> NPs, the hole nanostructure can behave as a siderophore, dragging the coordinated iron with MC inside the cell, MC behaves as the ionophore, which can disrupt the ion permeability of the cytoplasmic membrane. Previously we reported that nanostructuring of cefotaxime and ceftriaxone with magnetite NPs [19] significantly improves the antimicrobial effect of above-mentioned drugs, even on the resistant strains of *E. coli*. The continuation of our study [20] revealed the impressive synergistic effect of synthesized crown ether and cephalosporin antibiotics, united in magnetite based nanostructures, significantly decreasing the MIC of antimicrobial agents. Hopefully, bacteria will not soon be able to invent a new mechanism of resistance, against all the aspects of this nanostructures. Summarizing results of present and our previous studies, we can assume that synthesizing new supramolecular compounds, creating new nanostructures of antibiotics, coupled by Fe<sub>3</sub>O<sub>4</sub> NPs, and combining all these substances in nanoensembles can show significant results in the fighting against bacterial infections [19].

## Conclusion

The synthesis of compounds, having biological activity, and modification of already exist drugs for application in targeting drug delivery are among the key solutions of such problems as the resistance of microorganisms, the toxicity and adverse side effects of usual antibacterial agents. Our research's results show that the combining of supramolecular and nanotechnological approaches can make a great impact on antibacterial therapy. Synthesized hydroxyl substituted diazacrown shows a significant antibacterial effect and low MIC on gram-positive *S. aureus*, whereas nanostructured hydroxyl substituted azacrown produces an impressive effect and low MIC on gram-negative microorganism *K. spp.* and *E. coli*, and even has ability to inhibit their growth in biofilm almost in all concentrations.

## References

1. Steed, J.W., Atwood, J.L.: Supramolecular chemistry. 2nd edition, Chapter 1.7, pp. 27–38, Wiley, Hoboken (2009). ISBN: 978-0-470-51233-3
2. Cragg, P.J.: Supramolecular chemistry: from biological inspiration to biomedical applications. Springer, Heidelberg (2010). doi:

- 10.1007/978-90-481-2582-1, e-ISBN: 9789048125821; 9789048125814
3. Liu, L., Chen, S.: Theoretical study on cyclopeptides as the nanocarriers for  $\text{Li}^+$ ,  $\text{Na}^+$ ,  $\text{K}^+$  and  $\text{F}^-$ ,  $\text{Cl}^-$ ,  $\text{Br}^-$ . *J. Nanomater.* (2015). doi:[10.1155/2015/276191](https://doi.org/10.1155/2015/276191)
4. Jones, C.J., Thornback, J.R.: Medicinal applications of coordination chemistry, the royal society of chemistry. Chapter 4, pp. 203–205, (2007). ISBN: 978-0-85404-596-9
5. Nabeshima, T.:  $\text{Ag}^+$  selective macrocycles containing soft ligating moieties and regulation of  $\text{Ag}^+$  binding. *J. Incl. Phenom. Mol. Recognit. Chem.* **32**(2–3), 331–345 (1998). doi: [10.1023/A:1008079830979](https://doi.org/10.1023/A:1008079830979), Print ISSN: 0923-0750, Online ISSN: 1573-1111
6. Lehn, J.M.: Supramolecular chemistry concepts and perspectives. VCH, Weinheim (1995). ISBN: 3-527-29311-6 (Softcover), ISBN: 3-527-29312-4 (Hardcover)
7. Uskoković, V.: Nanostructured platforms for the sustained and local delivery of antibiotics in the treatment of osteomyelitis. *Crit. Rev. Ther. Drug Carr. Syst.* **32**(1), 1–59 (2015)
8. Dorniani, D., bin Hussein, M.Z., Kura, A.U., Fakurazi, S., Shaari, A.H., Ahmad, Z.: Preparation and characterization of 6-mercaptopurine-coated magnetite nanoparticles as a drug delivery system. *Drug Des. Dev. Ther.* **7**, 1015–1026 (2013). doi:[10.2147/DDDT.S43035](https://doi.org/10.2147/DDDT.S43035)
9. Grumezescu, A.M., Gestal, M.C., Holban, A.M., Grumezescu, V., Vasile, B.Ş., Mogoantă, L., Iordache, F., Bleotu, C., Mogoşanu, G.D.: Biocompatible  $\text{Fe}_3\text{O}_4$  increases the efficacy of amoxicillin delivery against gram-positive and gram-negative bacteria. *Molecules* **19**, 5013–5027 (2014). doi:[10.3390/molecules19045013](https://doi.org/10.3390/molecules19045013)
10. Latorre, M., Rinaldi, C.: Applications of magnetic nanoparticles in medicine: magnetic fluid hyperthermia. *Puerto Ric. Health Sci. J.* **28**(3), 227–238 (2009). ISSN: 0738-0658
11. Massart, R.: Preparation of aqueous magnetic liquids in alkaline and acidic media. *IEEE Trans. Magn.* **17**, 1247–1248 (1981). doi:[10.1109/TMAG.1981.1061188](https://doi.org/10.1109/TMAG.1981.1061188)
12. Mayrhofer, S., Domig, K.J., Mair, C., Zitz, U., Huys, G., Kneifel, W.: Comparison of broth microdilution, Etest, and agar disk diffusion methods for antimicrobial susceptibility testing of *Lactobacillus acidophilus* group members. *Appl. Environ. Microbiol.* **12**, 3745–3748 (2008). doi:[10.1128/AEM.02849-07](https://doi.org/10.1128/AEM.02849-07)
13. Jorgensen, J.H., Lee, J.C.: Microdilution technique for antimicrobial susceptibility testing of *Haemophilus influenza*. *Antimicrob. Agents Chemother.* **8**, 610–611 (1975). doi:[10.1128/AAC.8.5.610](https://doi.org/10.1128/AAC.8.5.610)
14. Erriu, M., Genta, G., Tuveri, E., Orrù, G., Barbato, G., Levi, R.: Microtiter spectrophotometric biofilm production assay analyzed with metrological methods and uncertainty evaluation. *Measurement* **45**, 1083–1088 (2012)
15. Grumezescu, A.M., Cotar, A.I., Andronescu, E., Ficai, A., Ghitulica, C.D., Grumezescu, V., Vasile, B.S., Chifiriuc, M.C.: In vitro activity of the new water-dispersible  $\text{Fe}_3\text{O}_4$  @usnic acid nanostructure against planktonic and sessile bacterial cells. *J. Nanopart. Res.* **15**, 1766 (2013). doi:[10.1007/s11051-013-1766-3](https://doi.org/10.1007/s11051-013-1766-3)
16. Tempelaars, M.H., Rodrigues, S., Abee, T.: Comparative analysis of antimicrobial activities of valinomycin and cereulide, the *Bacillus cereus* emetic toxin. *Appl Environ. Microbiol.* **77**(8), 2755–2762 (2011). doi:[10.1128/AEM.02671-10](https://doi.org/10.1128/AEM.02671-10)
17. Raymond, K.N.: Recognition and transport of natural and synthetic siderophores by microbes. *Pure Appl. Chem.* **66**(4), 773–781 (1994). doi:[10.1351/pac199466040773](https://doi.org/10.1351/pac199466040773)
18. Periasamy, S., Joo, H.S., Duong, A.C., Bach, T.H.L., Tan, V.Y., Chatterjee, S.S., Cheung, G.Y., Otto, M.: How *Staphylococcus aureus* biofilms develop their characteristic structure. *Proc. Natl. Acad. Sci.* **109**(4), 1281–1286 (2012). doi:[10.1073/pnas.1115006109](https://doi.org/10.1073/pnas.1115006109)
19. Hasanova, U.A., Ramazanov, M.A., Maharramov, A.M., Eyvazova, Q.M., Agamaliyev, Z.A., Parfyonova, Y.V., Hajiyeva, S.F., Hajiyeva, F.V., Veliyeva, S.B.: Nano-coupling of cephalosporin antibiotic with  $\text{Fe}_3\text{O}_4$  nanoparticles: trojan horse approach in antimicrobial chemotherapy of infections caused by *Klebsiella spp.*. *J. Biomater. Nanobiotechnol.* **6**, 225–235 (2015). doi:[10.4236/jbnb.2015.63021](https://doi.org/10.4236/jbnb.2015.63021)
20. Hasanova, U., Ramazanov, M., Maharramov, A., Gakhramanova, Z., Hajiyeva, S., Eyvazova, Q., Vezirova, L., Hajiyevaa, F., Hasanova, M., Guliyeva, N.: Synthesis of macrocycle (MC)—mimics the properties of natural siderophores and preparation the nanostructures on the basis of MC and magnetite nanoparticles. *CEt chem. Eng. Trans.* **47**, 109–114 (2016). doi:[10.3303/CET1647019](https://doi.org/10.3303/CET1647019)